Conf-910808--6

IRRADIATION-INDUCED SENSITIZATION AND STRESS CORROSION CRACKING OF TYPE 304 STAINLESS STEEL CORE-INTERNAL COMPONENTS*

H. M. Chung, W. E. Ruther, J. E. Sanecki, and T. F. Kassner

ANL/CP--74576

DE92 003380

Materials and Components Technology Division
Argonne National Laboratory
Argonne, IL 60439

August 1991

DISCLAIMER

Presented at the Fifth International Symposium on Environmental Degradation of materials in Nuclear Power Systems-Water Reactors, August 25-29, 1991, Monterey, CA.

*Work supported by the Office of Nuclear Regulatory Research, U.S. Nuclear Regulatory Commission.

IRRADIATION-INDUCED SENSITIZATION AND STRESS CORROSION CRACKING OF TYPE 304 STAINLESS STEEL CORE-INTERNAL COMPONENTS

H. M. Chung, W. E. Ruther, J. E. Sanecki, and T. F. Kassner

Materials and Components Technology Division
Argonne National Laboratory
Argonne, Illinois 60439 USA
Tel. 708-972-5111

ABSTRACT

High- and commercial-purity heats of Type 304 stainless steel, obtained from neutron absorber tubes after irradiation to fluence levels of up to 2 x 10^{21} n·cm^{-2} (E > 1 MeV) in two boiling water reactors, were examined by Auger electron spectroscopy to characterize irradiation-induced grain- boundary segregation and depletion of alloying and impurity elements. Segregation of Si, P, Ni, and an unidentified element or compound that gives rise to an Auger energy peak at 59 eV was observed in the commercial-purity heat. Such segregation was negligible in high-purity material, except for Ni. No evidence of S segregation was observed in either material. Cr depletion was more pronounced in the high-purity material than in the commercial-purity material. These observations suggest a synergism between the significant level of impurities and Cr depletion in the commercial-purity heat. In the absence of such synergism, Cr depletion appears more pronounced in the high-purity heat. Initial results of constant-extension-rate tests conducted on the two heats in air and in simulated BWR water were correlated with the results from analysis by Auger electron spectroscopy.

INTRODUCTION

In recent years, failures of core internal components in both boiling- and pressurized-water reactors (BWRs and PWRs) have increased after accumulation of relatively high fluence (>5 x 10^{20} n·cm^{-2}, E > 1 MeV). The general pattern of the observed failures indicates that as nuclear plants age and neutron fluence increases, a wide variety of apparently nonsensitized austenitic materials become susceptible to intergranular failure. Although most failed components can be replaced, some safety-significant structural components, such as the BWR top guide, shroud, and core plate, would be very difficult or impractical to replace. Therefore, the structural integrity of these components after accumulation of high fluence has been a subject of concern, and extensive research has been conducted to provide an understanding of this type of degradation process, commonly termed irradiation-assisted stress corrosion cracking (IASCC).[1-12]

Most of the safety-significant structural components are fabricated from solution-annealed austenitic stainless steels, primarily Type 304 stainless steel (SS). Component fabrication procedures and reactor operational parameters, such as neutron flux, fluence, temperature, water chemistry, and mechanical loads, have been reported as influencing susceptibility to IASCC.[1-12] However, research results from several laboratories on materials irradiated under a wide variety of simulated conditions are often inconsistent and conflicting as to the influence of these parameters.[4,11]

Failures of austenitic SS after accumulation of high fluence have been attributed to irradiation-induced sensitization in which radiation-induced segregation (RIS) or depletion of elements such as Si, P, S, Ni, and Cr at grain boundaries has been implicated. It is generally believed that the nonequilibrium process of RIS of impurity or alloying elements is strongly influenced by irradiation temperature and fast-neutron dose rate. However, the exact identity of the elements that segregate and the extent to which each segregated impurity or depleted element contributes to the enhanced susceptibility of core-internal components of to IASCC are not clear. This is particularly true

for Type 304 SS, from which the majority of the safety-significant in-core components have been fabricated, although RIS of impurity elements and grain-boundary depletion of Cr have been reported for Type 304 SS specimens irradiated under simulated conditions, i.e., either in test reactors[5,6,8] or by electrons[5] or ions.[10,12]

In view of the strong influences of irradiation temperature and dose rate, results obtained from simulation-irradiated specimens must be scrutinized carefully, and a benchmark analysis of actual reactor components must be obtained. For this purpose, high- and commercial-purity Type 304 SS specimens obtained from neutron absorber tubes of two operating BWRs have been analyzed and tested in this study.

The primary objective of this study is to determine the comparative characteristics of irradiation-induced sensitization in commercial- and high-purity heats of Type 304 SS during actual service in BWRs. The latter grade is a candidate material for mitigation of IASCC. Grain boundary microchemical modifications in the steels are also being correlated with results of separate tests in which comparative susceptibilities of the two grades to stress corrosion cracking (SCC) are being measured from slow strain-rate-tensile (SSRT) tests in simulated BWR water.

EXPERIMENTAL PROCEDURE

Type 304 SS was obtained from neutron absorber tubes that were irradiated in two BWRs. The tubes, containing B_4C absorber, were discharged from the reactors after several years of service. Fast neutron fluence and chemical compositions of the high- and commercial-purity (HP and CP) heats are given in Table 1. Compositions of the HP and CP heats were analyzed before and after service, respectively. C, B, P, and S contents of the CP material could not be obtained.

Analyses of grain-boundary microchemistry and irradiation-induced sensitization were conducted by Auger electron spectroscopy (AES) with a JEOL Company JAMP-10 Model scanning Auger microscope (SAM). Notched specimens (0.8 x 3.0 x 20 mm) were electropolished in a solution of phosphoric sulfuric acid (60:40% by volume). Each specimen was then charged with hydrogen for 45-50 h in an electrolyte of 0.1N sulfuric acid with 100 mg/L of arsenic pentoxide or sodium arsenide, both of which act as a hydrogen-recombination poisons. The hydrogen-charged specimens were fractured at room temperature in ultra-high vacuum (7 to 20 x 10^{-7} Pa) of the SAM. The freshly fractured surfaces were then examined without exposure to the atmosphere. After spectral analysis, depth profiles of alloying and impurity elements were obtained as a function of sputter distance beneath a selected region of intergranular fracture. The sputter (by Ar ion) removal rate was approximately 0.3-0.4 $nm \cdot s^{-1}$. Typically, a selected surface was sputtered for 2-4 s and then an Auger spectrum was obtained for 100-110 s on a fresh sputtered surface 1-2 s after the sputter removal of surface layers. The entire procedure was automated and computer-controlled.

RESULTS OF AES ANALYSIS

In general, intergranular fracture was relatively more difficult to produce in the HP specimens than in the CP specimens. Auger spectra characteristic of intergranular and ductile regions of a CP specimen are shown in Fig. 1. Overall spectra, as well as magnified plots of the low-energy regions of the spectra, are shown in Figs. 1A (obtained from intergranular region) and 1B (ductile), and Figs. 1C (intergranular) and 1D (ductile), respectively; the latter two better illustrate signals from impurity elements such as Si, P, and S.

Comparison of spectra characteristic of intergranular and ductile fracture surfaces, such as those in Fig. 1, revealed that (1) signals from O, C, and S are caused by contamination from the gaseous environment of the Auger microscope and that this contamination was consistently greater on ductile fracture surfaces than on intergranular surfaces, and (2) signals corresponding to Ni, P, Si, and an unidentified energy peak at 59 eV (denoted as $X_{59\text{-}eV}$) were stronger for an intergranular fracture surface than for a ductile surface.

To show these characteristics more quantitatively, Auger signals from several spots on ductile and intergranular fracture regions were analyzed, and peak-to-peak amplitudes of the primary peaks of Ni, Cr, Si, P, and the $X_{59\text{-}eV}$ peak were measured and normalized with respect to the amplitude of the 701-eV peak of Fe. The Cr peak height was strongly influenced by the adjacent O peak (Fig. 1) when Auger spectra were obtained from a unsputtered fracture surface. During a practical AES analysis, fractured surfaces are usually exposed to vacuum for a relatively long

Table 1. Chemical Compositions and Fluence of High- and Commercial-Purity Type 304 Stainless Steel BWR Absorber Rod Tubes

Material and Purity	Fluence Level, 10^{21} n/cm^2	Specimen Code	Composition (in wt.%)									
			Cr	Ni	Mn	C	N	B	Si	P	S	O
HP 304 SS[a]	1.4	VH	18.58	9.44	1.22	0.017	0.037	0.0002	0.02	0.002	0.003	–
	0.7	VM										
	0.2	VL										
CP 304 SS[b]	2.0	BL-H	16.80	8.77	1.65	–	0.052	–	1.55	–	–	0.024
	0.6	BL-M										
	0.2	BL-L										

[a]High-purity-heat neutron absorber, OD = 4.78 mm, wall thickness = 0.63 mm, chemical composition measured before service.
[b]Commercial-purity-heat absorber, OD = 4.78 mm, wall thickness = 0.79 mm, composition measured after service.

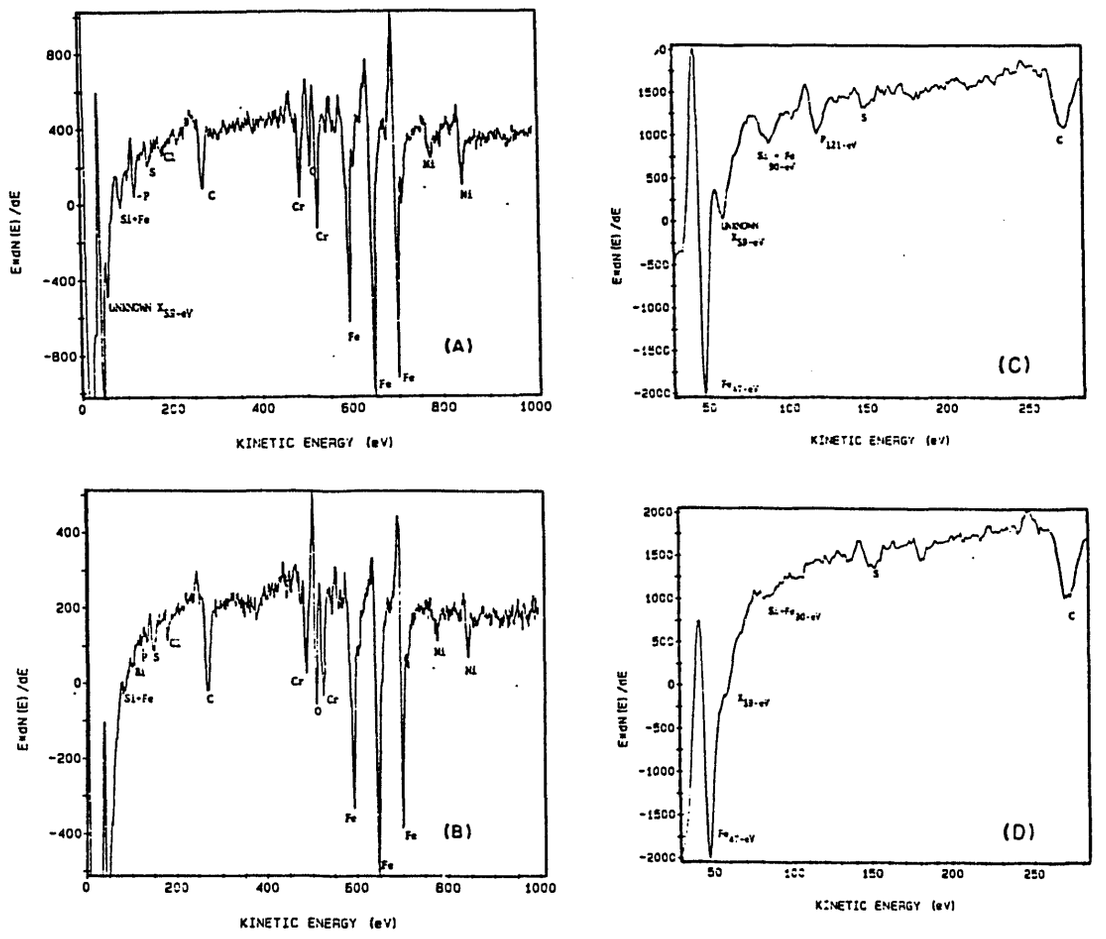

Fig. 1. Typical Auger spectra of an intergranular fracture surface (A); and ductile fracture surface (B) of commercial-purity Type 304 SS absorber tube irradiated to 2.0 x 10^{21} n/cm^2. (C) and (D) are expanded spectra of (A) and (B), respectively.

period (e.g., 0.5 h to several hours) before morphologies were examined and Auger spectra obtained. Apparently because of the O contamination associated with the long exposure, the Cr/Fe peak ratio decreased strongly with increased O/Fe peak ratio. This problem can be minimized when a fresh surface is examined immediately after sputter removal of surface layers.

Because of the characteristics of the Cr peak associated with analysis of unsputtered fracture surfaces, normalization with respect to the Fe peak was considered a better choice than normalization with respect to combined Fe, Ni, and Cr peaks. The normalized amplitudes shown in Figs. 2-4 correspond to the relative abundance of each element compared to the population of Fe atoms. These normalized amplitudes, obtained for ductile (denoted by "D") and intergranular ("I") surfaces of two CP specimens irradiated to a fluence of 2.0×10^{21} n cm^{-2}, are plotted in Figs. 2 and 3. In addition to these spectra from ductile and intergranular fracture regions, spectra were also obtained from featureless faceted fracture surfaces of uncertain morphology. This type of fracture surface is denoted by "U". Although the latter morphology indicated a nonductile fracture of the local area, it was not clear if it could be attributed to grain-boundary separation. However, the normalized amplitudes from intergranular fracture regions provide information on the relative concentration of elements on grain boundaries.

The Auger peak near 90 eV (Fig. 1) is composed of adjacent signals of Si (91 eV) and Fe (88 eV). However, the contribution from the 88-eV peak of Fe is relatively small (probably less than 3-5%,[8]), which can be surmised by comparing the peaks shown in Figs. 1C and 1D. Therefore, the normalized amplitude denoted as Si+Fe$_{90\text{-eV}}$ in Figs. 2 and 3 should correspond primarily to Si concentration. The peak at 59 eV could not be identified. It is possible that the 61-eV Ni peak could shift in both energy and amplitude because of the formation of a thin film of an Ni-Si compound (e.g., Ni- and Si-rich G phase) on the grain boundary. The 59-eV peak

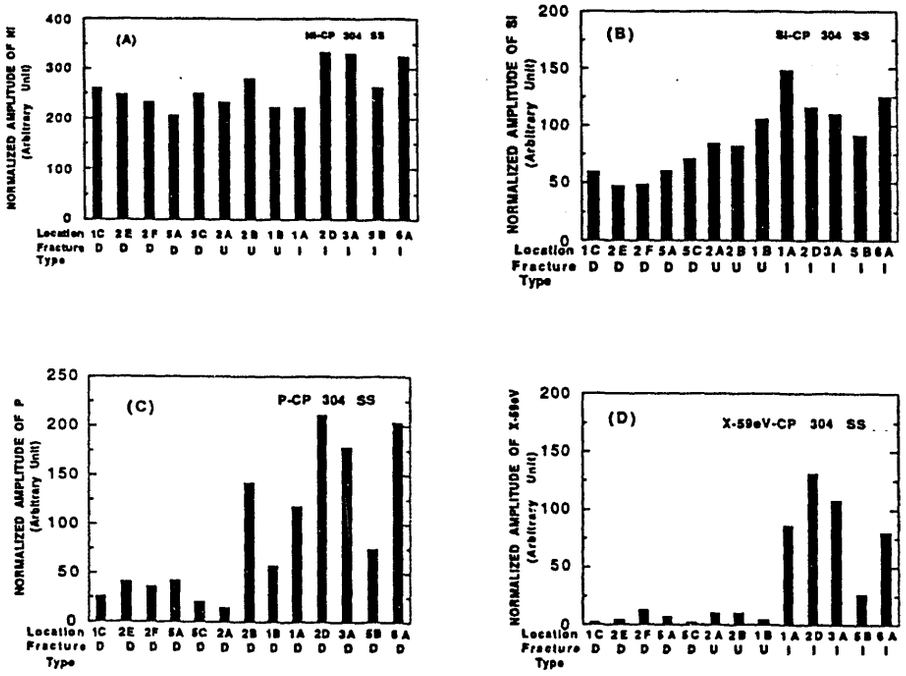

Fig. 2. Normalized peak-to-peak amplitudes of (A) Ni; (B) Si; (C) P; and (D) unidentified element (denoted as $X_{59\text{-eV}}$ in Fig. 1) that were obtained from ductile (denoted by letter D), intergranular (I), and uncertain faceted (U) fracture surfaces of a commercial-purity absorber tube specimen irradiated to a fluence of 2.0×10^{21} n/cm^2.

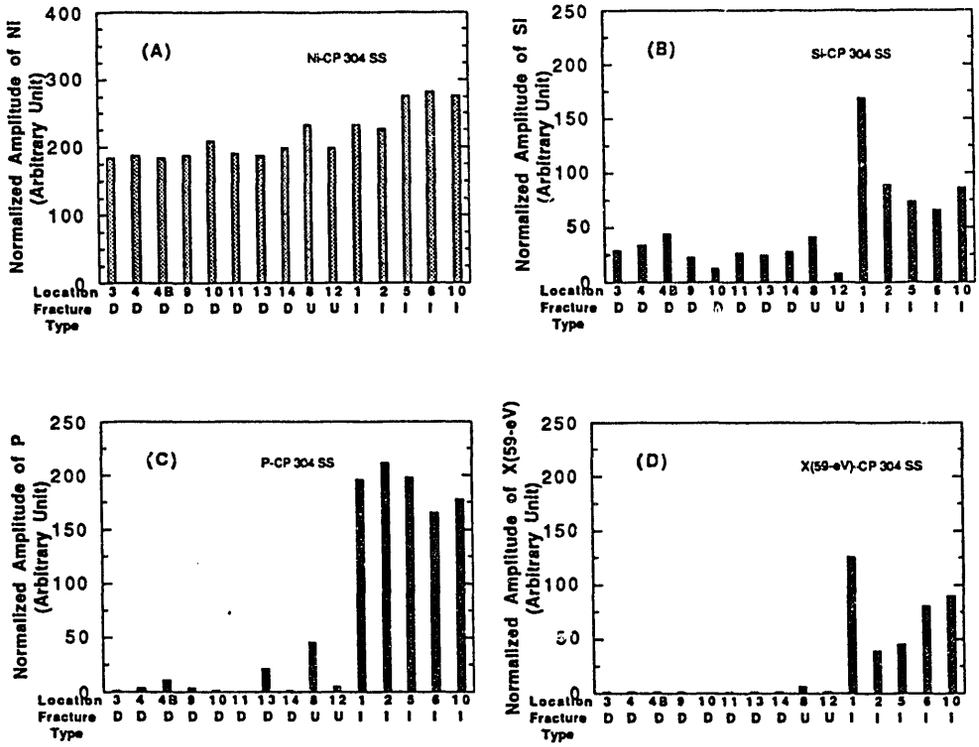

Fig. 3. Normalized amplitudes similar to those in Fig. 2 obtained from another commercial-purity absorber tube specimen irradiated to 2.0 x 10^{21} n/cm^2.

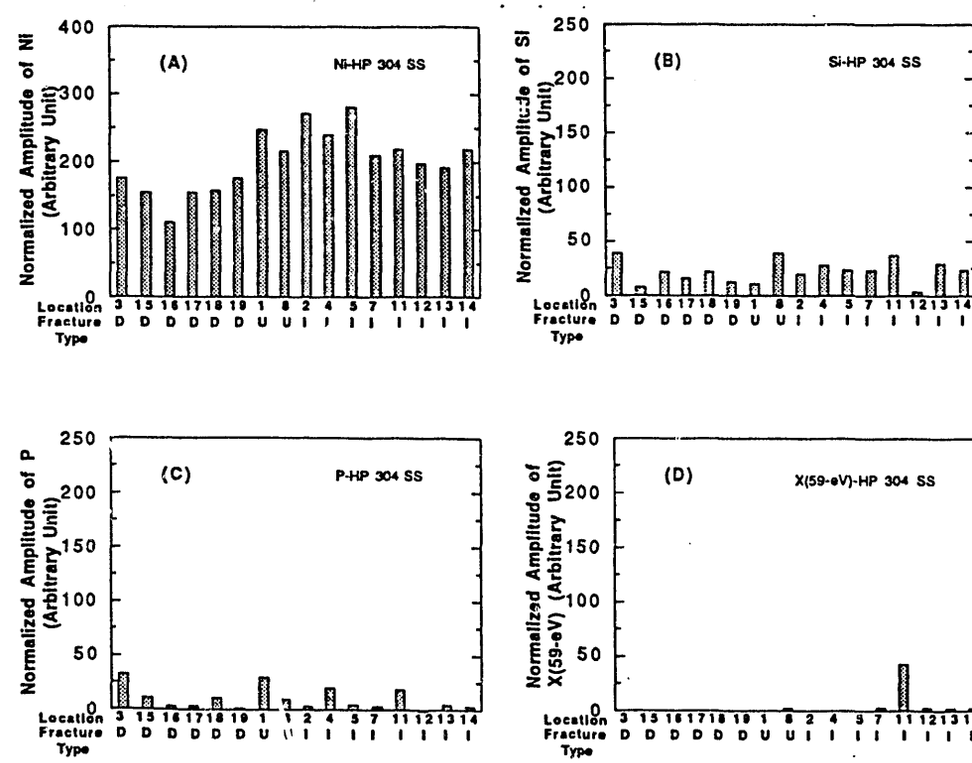

Fig. 4. Normalized amplitudes similar to those in Figs. 2 and 3, obtained from a high-purity absorber tube specimen irradiated to 1.4 x 10^{21} n/cm^2.

amplitude was proportional to the amplitudes of the Si peak (but not proportional to the Ni peak) and was significant only on intergranular fracture surfaces of the CP specimens.

From Figs. 2 and 3, the relative segregation of each element can be determined. It can be concluded from the figures that Ni, Si, and P atoms segregate to grain boundaries in a CP specimen. Although the 59-eV peak could not be identified at this time, Figs. 2 and 3 also indicate that intergranular fracture of a CP specimen is associated with the high intensity of this peak.

Results similar to those of Figs. 2 and 3 but obtained for an HP specimen irradiated to a fluence of 1.4×10^{21} n cm^{-2}, are plotted in Fig. 4. In distinct contrast to those of CP specimens, the results in Fig. 4 show no evidence of segregation of Si, P, or the 59-eV peak. Intensities of S, C, and O from intergranular surfaces were relatively higher in HP than in CP specimens, indicating relatively more contamination on the cleaner intergranular surfaces of the HP specimen than on those of the CP specimen. Thus, it was clear that no significant segregation of impurity elements occurred during irradiation of the HP specimens.

However, grain-boundary segregation of Ni was more pronounced in the HP (segregation ratio 1.5) than in the CP specimens (segregation ratio 1.3). This is shown in Fig. 5.

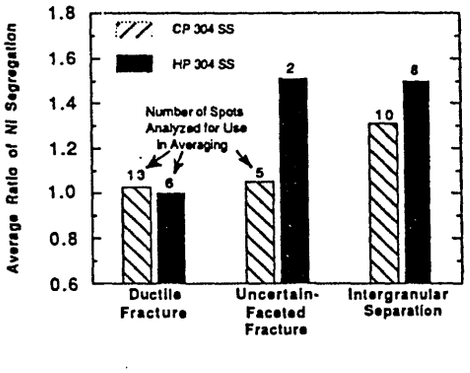

Fig. 5. Comparison of average ratios of Ni segregation on 3 types of fracture surfaces (ductile, uncertain-faceted, and intergranular separation) for commercial- and high-purity absorber tube specimens of Figs. 2-4.

In general, the intensity of the S peak was stronger in a specimen that was fractured following the hydrogen-charging and Cu-plating procedure than in a specimen fractured without the Cu-plating step. Apparently, higher S contamination occurred during Cu plating because a S-containing solution was used in the Cu-plating process.

As pointed out above, distribution of Cr near a grain boundary could be characterized better by the sputter depth-profile technique. As expected, the grain boundaries in both CP and HP specimens were depleted of Fe and Cr and enriched in Ni. The Cr distributions in Fig. 6 were obtained by sputtering three intergranular fracture surfaces of CP specimens irradiated to a fluence of 2.0×10^{21} n cm^{-2}. Relatively low depletion ratios of 0.75-0.87 were observed in the CP specimens.

Cr depletion profiles, similar to Fig. 6 but obtained from two specimens of the HP heat, are shown in Fig. 7. The shapes of the two Cr-depletion profiles in Fig. 7 differ. Contrasting shapes similar to those in the figure have been also reported from analysis by field-emission-gun scanning transmission electron microscopy (FEG-STEM).[10] Figures 6 and 7 indicate that Cr depletion is more pronounced in the HP heat (depletion ratios of 0.40-0.52) than in the CP heat (depletion ratios of 0.75-0.87). These depletion ratios correspond to

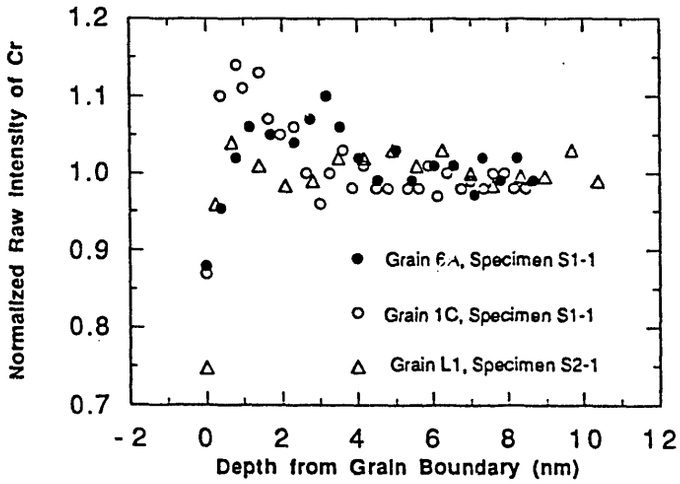

Fig. 6. Comparison of grain-boundary profiles of Cr obtained underneath three intergranular-fracture surfaces from two commercial-purity absorber tube specimens irradiated to 2.0×10^{21} n/cm^2.

grain-boundary Cr contents of 8-9 and 13-15 wt.%, respectively, for the HP and CP specimens.

More direct comparisons of the characteristics of Cr depletion in the HP and CP materials are shown in Fig. 8. The comparison of Fig. 8A is based on the raw-intensity data from Grain Boundaries 6A, Fig. 6 (CP heat) and L13, Fig. 7 (HP heat). A similar comparison (Fig. 8B) is based on the raw-intensity data from Grain Boundaries L1, Fig. 6 (CP heat) and C1, Fig. 7 (HP heat). From overall depth-profile data, i.e., raw intensities and sensitivity factors of Fe, Ni, O, C, S, P, Si, Cl, and Cr, the Cr contents corresponding to Fig. 8B were then converted to at.%. The comparison shown in Fig. 8C is based on at.% Cr. The two comparisons obtained from the two identical sets of data, i.e., Figs. 8B (in raw intensity) and 8C (in at.%), are essentially similar. This further confirms that Cr depletion is more pronounced in the HP heat than in the CP heat. In general, grain-boundary Cr depletion profiles in the HP specimens are deeper and wider than those in the CP specimens.

DISCUSSION

The AES analyses show that undersize atoms, namely, Si, P, and Ni, segregate to grain boundaries, whereas oversized atoms, namely Cr, diffuse away from grain boundaries. This seems to be qualitatively consistent with theory[7] and FEG-STEM observations reported for electron- and test-reactor-irradiated[5] and ion-irradiated Type 304 SS[10] and BWR-irradiated Type 348 SS.[9,10]

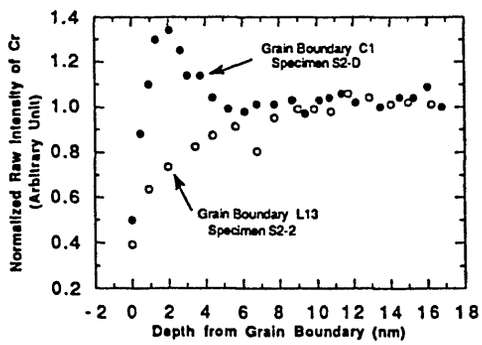

Fig. 7. Comparison of grain-boundary profiles of Cr obtained underneath two intergranular fracture surfaces from two HP absorber tube specimens irradiated to a fluence of 1.4×10^{21} n/cm^2

A previous AES study on CP Type 304 SS irradiated in the Advanced Test Reactor indicated that S was the major element that segregated to grain boundaries.[8] Si and P were reported in the study to be secondary impurities that segregated. A recent study by AES and FEM-STEM on BWR-irradiated Type 348 SS, however, indicated that Si is the

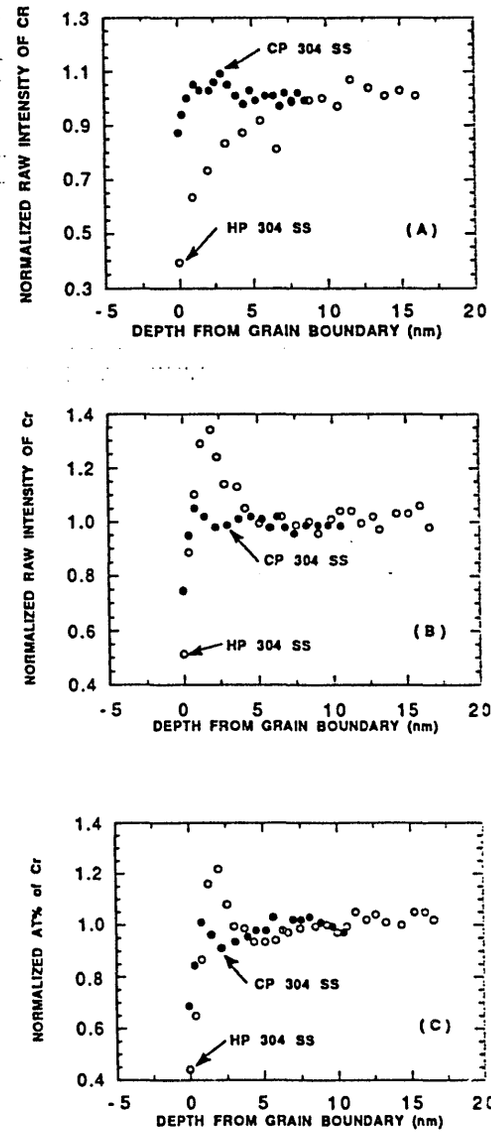

Fig. 8. Comparisons of Cr depletion profiles of CP and HP absorber tubes; (A) comparison of raw-intensity data from Grain Boundaries 6A, Fig. 6 and L13, Fig. 7; (B) comparison of raw-intensity data from Grain Boundaries L1, Fig. 6 and C1, Fig. 7; (C) similar to (B) in at.% Cr.

primary impurity that segregates, while segregation of P is secondary.[9] The result from the former study[8] is in direct contrast to the present results obtained from the CP specimens, in which no evidence of S segregation was observed. Sulfur should be detected by FEG-STEM; however, no evidence of S segregation has been reported from such investigations of BWR-irradiated Type 348 SS[9] or 304 SS.[10] In view of this, S segregation and a role of S in IASCC of Type 304 SS in BWR environments are considered unlikely.

Evidence of P segregation has been reported previously for Type 304 SS irradiated at 300°C in test reactors,[5,8] by electrons,[5] and by ions,[10] and for Type 348 SS irradiated in a BWR.[9] The results in Figs. 2C and 3C are consistent with these observations.

The relatively easy intergranular fracture of the hydrogen-charged CP specimens in vacuo in the present study seems to be associated with significant segregation of Si, P, and the unidentified element or compound that gives rise to the 59-eV peak ($X_{59\text{-}eV}$). A synergistic interaction between Si and Ni segregated on grain boundaries, which may lead to formation of a thin film of G-phase or other Ni-Si compound, cannot be ruled out. The G phase, a phase rich in Ni and Si and having a composition close to $(Fe,Cr,Mn)_6Ni_{17}Si_7$, was observed both on and away from grain boundaries of Type 316 SS irradiated at 480 to 530°C by fast neutrons in EBR-II.[13] A significant weakening of grain boundaries may occur as a result of such thin-film formation.

The absence of significant segregation of impurity elements on grain boundaries of the HP Type 304 SS specimens is obviously a result of the very low impurity content. However, despite negligible impurity segregation, Cr depletion was more pronounced in the HP specimen than in the CP material for a similar fluence level. This suggests a synergism between Cr depletion and impurity segregation (i.e., reduced Cr depletion accompanying a pronounced impurity segregation). The two groups of oversized atoms (Cr) and undersized atoms (Si and P) diffuse in opposite directions, i.e., away from and toward grain boundaries, respectively. In this simultaneous process, mobility of Cr atoms that diffuse away from grain boundaries by jumping preferentially to vacancies may be perturbed by the incoming flux of interstitial-Si and interstitial-P complexes, which thereby suppresses Cr depletion in the CP material. Another possibility is that the higher impurity content in the grains of the CP heat is conducive to more pronounced formation of vacancy sinks such as dislocation loops and "black-dot defects," resulting in a less pronounced vacancy flux from midgrain to grain boundaries. This would result in reduced depletion of oversize atoms such as Cr.

CORRELATION WITH INITIAL RESULTS FROM SSRT TESTS

If Cr depletion is the primary mechanism that controls SCC, HP specimens would be expected to exhibit a greater susceptibility to SCC than CP materials. If impurity segregation is the primary mechanism, the opposite result is expected. To clarify these contrasting alternatives to the IASCC process, SSRT tests are being conducted in a hot-cell facility on tube specimens from the two heats of Type 304 SS in air and in simulated BWR water.

Initial results on the CP and HP materials for a strain rate of 1.65×10^{-7} s^{-1} at 289°C are summarized in Table 2. Dissolved oxygen content and conductivity of the simulated BWR water were 280 ppb and 0.13 μS cm^{-1}, respectively. The high initial stress on the specimens tested in water results from the pressure of the high-temperature water acting on the cross-sectional area of the pull rod in the autoclave sliding seal. Because the cross-sectional area of the pull rod is large compared to that of the absorber tube specimen, the initial stress exerted on the tube specimen was high. Figure 9 shows four sets of comparisons of stress versus elongation for CP and HP specimens strained to failure in air and in water containing 280 ppb dissolved oxygen (see Table 2). Yield and ultimate tensile strengths of the HP absorber tubes tested in air (Figs. 9C and 9D) are comparable to those reported for Type 304 and 304L SS irradiated to similar fluences in the Advanced Test Reactor.[14] However, yield and ultimate strengths obtained for the CP heat are somewhat lower than the values reported for similar fluence levels in the same study.[14] For a comparable fluence level, ductility of the HP heat seems to be significantly lower than that of the CP heat.

Shorter times to failure, lower maximum stress, and smaller elongation to failure of the specimens tested in water are indicative of significant SCC of the high- and medium-fluence specimens (i.e., specimens with fluence $>0.6 \times 10^{21}$ n cm^{-2}, E > 1 MeV). For a

Table 2. Slow Strain Rate[a] Tensile Test Results on Irradiated Commercial- and High-Purity Type 304 SS in Air and in High-Purity Water Containing 280 ppb Dissolved Oxygen at 289°C

Absorber Rod Specimen No.	Hot-cell Section No.	Fast-Neutron Fluence, $n \cdot cm^{-2}$	Feedwater Chemistry			SSRT Parameters		
			Oxygen Conc., ppb	Cond. at 25°C $\mu S \cdot cm^{-1}$	pH at 25°C	Failure Time, h	Maximum Stress, MPa	Total Elong., %
BL-BWR-2H	389E1A	0.2×10^{21}	air	air	air	260	390	15.6
BL-BWR-2H	389E1D	0.2×10^{21}	280	0.13	6.23	107	337	6.7
BL-BWR-2M	389E2D	0.6×10^{21}	air	air	air	580	465	34.8
BL-BWR-2M	389E2A	0.6×10^{21}	290	0.15	6.32	140	359	8.3
BL-BWR-2L	389E3A	2.0×10^{21}	air	air	air	228	631	13.5
VH-A7A-L2	406A1	1.4×10^{21}	air	air	air	93	786	5.6
VH-A7A-L1	-	1.4×10^{21}	280	0.10	6.28	11	417	0.6
VM-D5B-L2	-	0.7×10^{21}	air	air	air	405	684	24.2
VM-D5B-L1	-	0.7×10^{21}	280	0.12	6.26	31	552	1.8

[a]Strain rate of $1.65 \times 10^{-7}\ s^{-1}$.

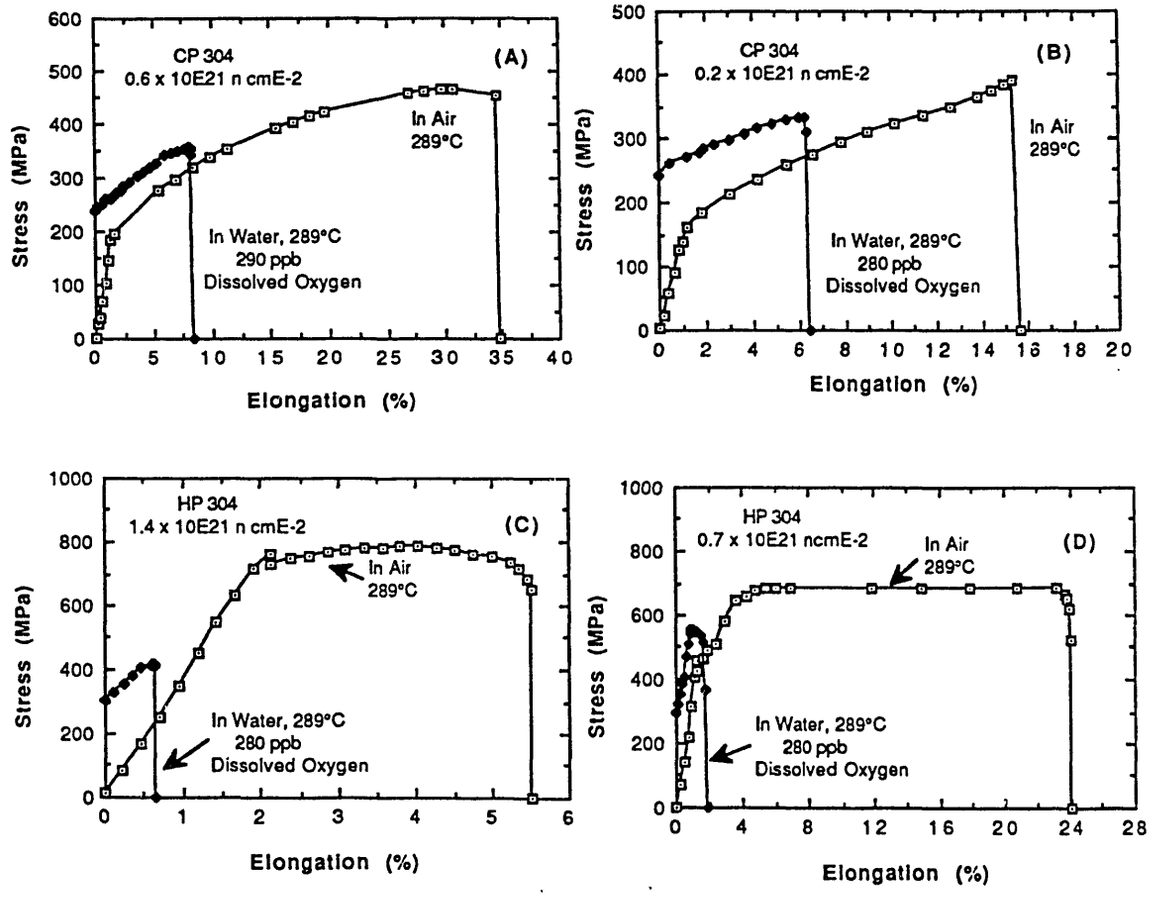

Fig. 9. Comparison of stress versus elongation from SSRT tests at 289°C in air and in high-purity water simulating BWR environment; (A) CP Type 304 SS absorber tube irradiated to 0.6×10^{21} n cm^{-2}; (B) CP tube irradiated to 0.2×10^{21} n cm^{-2}; (C) HP tube irradiated to 1.4×10^{21} n cm^{-2} ; (D) HP tube irradiated to 0.7×10^{21} n cm^{-2} .

similar fluence level of 0.6×10^{21} to 0.7×10^{21} n cm^{-2}, a comparison of Figs 9A and 9D indicates that the effect of the water environment in promoting SCC is more pronounced in the HP specimen (Fig. 9D) than in the CP specimen (Fig. 9A). The HP specimen irradiated to 1.4×10^{21} n cm^{-2} and tested in water (Fig. 9C) exhibited intergranular fracture morphology on 58% of the fracture surface (Fig. 10). Rate of the intergranular crack growth in Fig. 10 is estimated to be 1.6×10^{-8} m/s. It is difficult to explain the significant intergranular SCC in this specimen on the basis of Si or P segregation because impurity segregation in the HP heat was negligible for all fluence levels (Fig. 4). Rather, it seems consistent with a mechanism that irradiation-induced Cr depletion is the primary process, at least for an environment similar to the present simulated BWR water. However, in case of a significantly different water chemistry, one cannot rule out a possibility that Si or P segregation plays an important role. Probably, an extreme example of this manifestation of environmental effect is the observation that intergranular fracture was consistently easier to produce in CP specimens than in HP specimens in AES environment following the comparable hydrogen charging. If grain boundary microchemistry similar to those of the hydrogen-charged CP specimens is produced in or out of reactor by some process (e.g., excessive hydrogen uptake either from corrosion or from transmutation), the material is likely to be susceptible to intergranular failure largely independent of environment. It is possible that the intergranular fracture surfaces produced in argon atmosphere in PWR-irradiated commercial-purity Type 304 SS, reported in Ref. 15, could be related to a similar process.

Because of limited SSRT results obtained to date, a conclusive statement on relative resistance to IASCC of the HP and CP heats cannot be made at this time. To determine IASCC susceptibilities of the two heats more quantitatively, SSRT tests and fractographic analysis are being conducted further.

CONCLUSIONS

1. Irradiation-induced sensitization in high- and commercial-purity (HP and CP) Type 304 SS neurton absorber tubes, irradiated in two BWRs to fluences of 1.4 to 2.0 x 10^{21} n·cm^{-2} (E > 1 MeV), was characterized by AES. Significant irradiation-induced segregation of Si, P, Ni, and an unidentified element or compound that gives rise to an Auger energy peak at 59 eV was observed on grain boundaries of commercial-purity Type 304 SS. Such segregation was

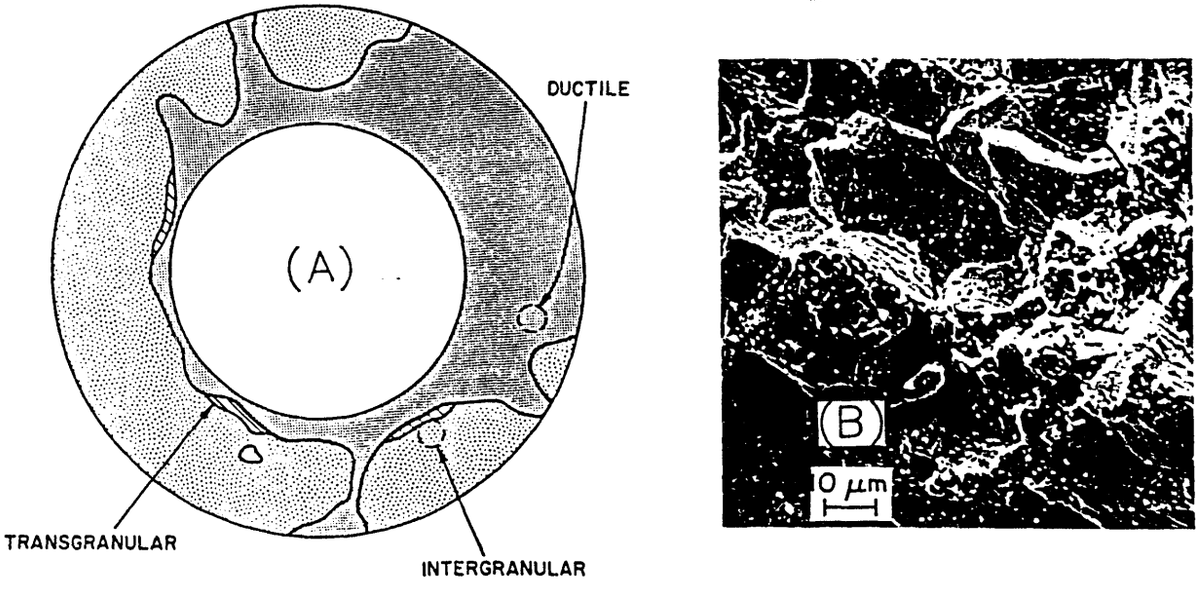

Fig. 10. Schematic (A) of composite fracture surface morphologies of the HP specimen irradiated to 1.4×10^{21} n cm^{-2} and tested in water, and morphology (B) of the encircled intergranular area in (A).

negligible in HP material, except for Ni. No evidence of S segregation was observed in either HP or CP heat.

2. Cr distribution near grain boundaries could be determined successfully only by sputtering and depth-profile technique. Cr depletion from grain boundaries was more pronounced in the HP heat than in the CP heat. Coupled with the previous conclusions, this suggests a synergism between Si and P segregation and Cr depletion in the CP material.

3. Initial results from slow-strain-rate tests showed significant intergranular SCC in the HP heat, indicating that Si or P segregation did not play an important role (at least directly) but that Cr depletion played a critical role in the simulated BWR water.

ACKNOWLEDGMENTS

The authors are grateful to D. Donahue, G. Dragel, and G. Talaber for specimen preparation and hot-cell SSRT tests. The irradiated BWR components were obtained with the assistance of R. Kohli, A. J. Jacobs, and J. L. Nelson. The authors thank W. J. Shack and J. Muscara for their helpful discussions. This work was supported by the Office of Nuclear Regulatory Research, U.S. Nuclear Regulatory Commission.

REFERENCES

1. W. L. Clark and A. J. Jacobs, Proc. 1st Intl. Symp. Environmental Degradation of Materials in Nuclear Power Systems - Water Reactors, National Association of Corrosion Engineers, 1984, pp. 451-461.

2. F. Garzarolli, D. Alter, and P. Dewes, Proc. 2nd Intl. Symp. Environmental Degradation of Materials in Nuclear Power Systems - Water Reactors, National Association of Corrosion Engineers, 1986, pp. 131-138.

3. F. Garzarolli, D. Alter, P. Dewes, and J. L. Nelson, Proc. 3rd Intl. Symp. Environmental Degradation of Materials in Nuclear Power Systems - Water Reactors, G. J. Theus and J. R. Weeks, Eds., The Metallurgical Society, Warrendale, PA, 1988, pp. 657-664.

4. H. Hanninen and I. Aho-Mantila, ibid., pp. 77-92.

5. K. Fukuya, S. Nakahigashi, S. Ozaki, M. Teresawa, and S. Shima, ibid., pp. 665-671.

6. A. J. Jacobs, G. P. Wozaldo, K. Nakata, T. Yoshida, and I. Masaoka, ibid., pp. 673-681.

7. E. P. Simonen and R. H. Jones, ibid., 683-690.

8. A. J. Jacobs, R. E. Clausing, L. Heatherly, and R. M. Kruger, Effects of Radiation on Materials: 14th Intl. Symp., Vol. I, ASTM STP 1046, N. H. Packan, R. E. Stoller, and A. S. Kumar, Eds., American Society for Testing and Materials, Philadelphia, 1989, pp. 424-436.

9. A. J. Jacobs, R. E. Clausing, M. K. Miller, and C. Shepherd, Proc. 4th Intl. Symp. Environmental Degradation of Materials in Nuclear Power Systems - Water Reactors, Jekyll Island, GA, Aug. 6-10, 1989, pp. 14-21 to 14-45.

10. C. M. Shepherd and T. M. Williams, ibid., pp. 14-11 to 14-20.

11. P. L. Andresen, F. P. Ford, S. M. Murphy, and J. M. Perks, ibid., pp. 1-83 to 1-121.

12. S. Bruemmer, L. Charlot, and E. Simonen, Proc. Corrosion 90, National Association of Corrosion Engineers, April 1990, Paper No. 506.

13. W. J. S. Yang, Radiation-Induced Changes in Microstructure: 13th Intl. Symp., ASTM STP 955, F. A. Garner, N. H. Packan, and A. S. Kumar, Eds., American Society for Testing and Materials, Philadelphia, 1987, pp. 628-646.

14. A. J. Jacobs, G. P. Wozaldo, K. Nakata, T. Yoshida, and I. Masaoka, Proc. 3rd Intl. Symp. Environmental Degradation of Materials in Nuclear Power Systems - Water Reactors, G. J. Theus and J. R. Weeks, Eds., The Metallurgical Society, Warrendale, PA, 1988, pp. 673-681.

15. M. P. Manahan, R. Kohli, J. Santucci, P. Sipush, and R. L. Harris, Proc. 9th Intl. Conf. on Structural Mechanics in Reactor Technology, Aug. 17-21, 1987, Lausanne, Switzerland.

END

DATE FILMED

12/31/91